Protein Science (1995), *4*:1758–1767. Cambridge University Press. Printed in the USA.

Structure and function of microplasminogen: I. Methionine shuffling, chemical proteolysis, and proenzyme activation

JIEYI WANG,[1] B. BRDAR,[2] AND E. REICH

Department of Pharmacological Sciences, SUNY at Stony Brook, Stony Brook, New York 11794-8651

(RECEIVED October 31, 1994; ACCEPTED June 15, 1995)

Abstract

We have cloned and expressed microplasminogen (*mPlg*), consisting of the N-terminal undecapeptide of human glu-*Plg* spliced to its proenzyme domain. This truncated (~28 kDa) proenzyme retained the distinctive catalytic activities of the larger parent. Replacement of M residues followed by M shuffling permitted subsequent scission by site-directed chemical proteolysis (in CNBr/formic acid) without impairing any of the protein's characteristic properties. Activation of chymotrypsinogen-related zymogens occurs by limited proteolysis; the newly liberated, highly conserved N-terminus (VVGG) forms a salt bridge with an aspartyl residue immediately upstream of the active site serine. The role of both of these elements in *mPlg* activation was probed using protein engineering and site-directed proteolysis to alter the length and amino acid composition of the N-terminus, and to replace the aspartate. All modifications affected both K_m and k_{cat}. The results identify some structural parameters of the N-terminus required for proenzyme activation.

Keywords: methionine shuffling; microplasminogen; proenzyme activation; protein engineering; serine proteases; site-directed proteolysis; zymogen activation; plasminogen activation

Plasminogen and its activated form, plasmin, belong to the chymotrypsin(ogen) family of serine proteases, a group of enzymes normally activated by limited proteolysis at a single defined position of the polypeptide chain. Crystallographic and other studies of chymotrypsinogen, trypsinogen, and their active derivatives (Freer et al., 1970; Birktoft & Blow, 1972; Fehlhammer et al., 1977; Kossiakoff et al., 1977; Huber & Bode, 1978) have shown that the new N-terminal segment liberated by chain cleavage (whose sequence is highly conserved within the chymotrypsinogen family) reorients and enters a pocket where its α-amino group forms a salt bridge with an aspartate residue that is the nearest upstream neighbor of the serine at the active site. *Plg* is an advantageous proenzyme for exploring the role of the salt-bridge mechanism and the importance of the constituent residues because (1) it can be activated both with and without chain cleavage and (2) its activation site is located within a small disulfide loop that constrains the structure and properties of the newly generated N-terminal segment.

To explore the mechanisms of proenzyme activation and other interesting facets of *Plg*, such as the basis of substrate specificity for *PA*s and the nature of the complexes with *SK*, it would be useful to assess the effects of structural perturbations produced by cleavages introduced at different positions in the *Plg* sequence. For this purpose, the polypeptide chain would require incision at locations that were both unique and different to the normal cleavage site. Lacking the necessary enzymes, we have achieved site-directed proteolysis by combining methionine shuffling with protein engineering, permitting unique scission of polypeptide chains at any desired site(s).

Our experiments have been performed on a truncated form of human *Plg*, microplasminogen, consisting essentially of the proenzyme domain (see Materials and methods), because it offers the convenience of reduced size while retaining most of the distinctive characteristics of the native protein.

Reprint requests to: E. Reich, Department of Pharmacological Sciences, SUNY at Stony Brook, Stony Brook, New York 11794-8651; e-mail: ed@pharm.som.sunysb.edu.

[1] Present address: Abbott Laboratories, Abbott Park, Illinois 60064.

[2] Present address: Ruder Boskovic Institute, Department of Molecular Genetics, 41001 Zagreb, P.O. Box 1016, Bijonicka 54, Croatia.

Abbreviations: BSA, bovine serum albumin; CNBr/HFo, cyanogen bromide in 73.5% formic acid; *PA*, plasminogen activator; *tPA*, tissue plasminogen activator; *uPA*, urokinase; *b-Plg*, bovine plasminogen; *b-Plm*, bovine plasmin; glu-*Plg*, plasminogen with glutamic acid N-terminus; *Plg*, plasminogen; *Plm*, plasmin; *mPlg*, microplasminogen; *mPlm*, microplasmin; *mPlgM*$^-$, methionineless microplasminogen; *mPlmM*$^-$, methionineless microplasmin; *mPlg-SK mPlm-SK*, the streptokinase complexes of microplasminogen and microplasmin, respectively; *SK*, streptokinase; PBS, phosphate-buffered saline. Amino acids are represented by the single-letter code.

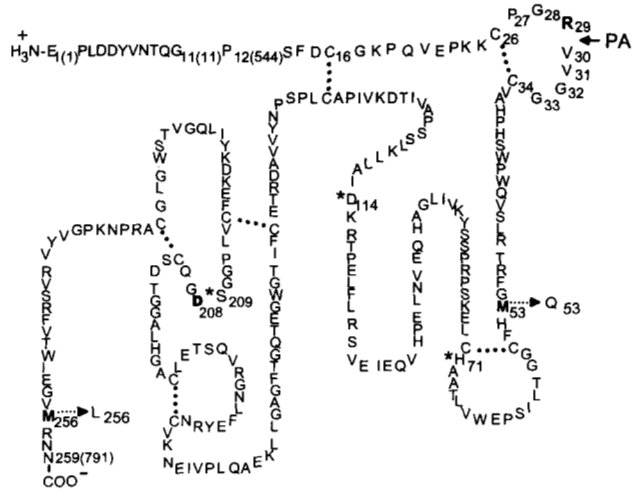

Fig. 1. Diagram of human microplasminogen (variant 1). Numbers in parentheses refer to the residue positions in glu-*Plg*. $H_{71}D_{114}S_{209}$ is the catalytic triad; D_{208} is the aspartyl upstream neighbor of the active site serine. The disulfide bonds are shown; the bond cleaved by plasminogen activators (R_{29}–V_{30}) is indicated, as are the positions of M substitutions to obtain *mPlgM*$^-$ (variant 4). This *mPlg* differs from the proteolytic product reported by Shi and Wu (1988).

Site-directed proteolysis was performed by methionine shuffling, that is, by substituting M at the desired position in the polypeptide chain and cleaving with CNBr in 73.5% formic acid (Gross & Witkop, 1961). To obtain a protein structure suitable for this procedure, the two M residues in *mPlg* (M_{53} and M_{256}) were first replaced, respectively, by Q and L, to yield two monomethionine forms; one of these was used to generate a completely methionineless protein and, thereby, a favorable context for engineering any desired pattern of site-specific M introduction and subsequent chain scission. Here we show that methionineless *mPlgM*$^-$ tolerates the conditions of chemical cleavage without loss or impairment of its characteristic catalytic properties.

Table 1. *Microplasminogen and mutant forms*[a]

Variant no.	Variant no.
1 $M_{53,256}$-*mPlg*	11* M_{31}, $G_{32a,32b}$, Q_{53}, L_{256}
2 Q_{53}, M_{256}	12 P_{30}, $M_{53,256}$
3 M_{53}, L_{256}	13* M_{29}, P_{30}, Q_{53}, L_{256}
4 Q_{53}, L_{256}-*mPlgM*$^-$	14* M_{30}, K_{31}, Q_{53}, L_{256}
5* M_{29}, Q_{53}, L_{256}	15 G_{32a}, $M_{53,256}$
6* M_{28}, Q_{53}, L_{256}	16 ΔV_{30}, $M_{53,256}$
7* M_{30}, Q_{53}, L_{256}	17 ΔG_{32}, $M_{53,256}$
8* M_{31}, Q_{53}, L_{256}	18 ΔV_{30}, ΔG_{32}, $M_{53,256}$
9* M_{30}, G_{32a}, Q_{53}, L_{256}	19 M_{53}, N_{208}, M_{256}
10 G_{30}, $M_{53,256}$	20 M_{53}, A_{208}, M_{256}

$C_{26}P_{27}G_{28}R_{29}{}'V_{30}V_{31}G_{32}G_{33}C_{34}$

[a] Individual designations show the position, if any, of all methionine residues, as well as mutational changes involving any site in each protein. * Identifies variants designed for chemical cleavage. Subscripts a and b represent residue insertion at the indicated position. Δ denotes deletion of the indicated residue. The amino acid sequence within the disulfide-bonded activation loop and the site of activating cleavage are shown for reference.

Results

Cloning, expression, purification, and characterization of mPlg, mPlgM$^-$*, and derivatives*

Figure 1 presents the amino acid sequence and disulfide architecture (Sottrup-Jensen et al., 1978) of *mPlg*; the sequence changes considered in this section are listed in the accompanying Table 1 and are four in number: two monomethionine replacements (variants 2 and 3); the methionineless protein *mPlgM*$^-$, variant 4; and the $R_{29} \rightarrow M_{29}$ mutation at the activation site, in the *mPlgM*$^-$ background (variant 5).

Progressive methionine removal from mPlg

The two monomethionine variants (2 and 3) were expressed in *Escherichia coli* and in High Five cell cultures, the respective proteins purified, and their interactions with *uPA* and *SK* assayed zymographically (Granelli-Piperno & Reich, 1978). By these measures, the two proenzymes appeared indistinguishable from wild-type *mPlg* in electrophoretic mobility and in observable caseinolytic activity generated by *uPA* and *SK*.

The methionineless variant (*mPlgM*$^-$ variant 4) was first expressed in *pMal-p* with an M residue at the fusion site between *mPlg* and the *malE* maltose binding protein. The periplasmic proteins were prepared (Riggs, 1990), incubated with CNBr/HFo, and the progress of fusion protein fragmentation followed as a function of time by SDS-PAGE and zymography (Fig. 2). Fragmentation of the fusion protein was initiated predominantly at M residues within the *malE* fusion partner, producing zymographically visible bands migrating with mobility intermediate between the fusion protein (~75 kDa) and *mPlg* (~37 kDa)[3]; these species then declined with progressive liberation and accumulation of a band indistinguishable from *mPlg* itself. The enzymatic activity of *mPlg* had clearly survived exposure to CNBr/HFo.

Purification of mPlg

Because *mPlg* lacked all kringle structures, it could not be isolated by the familiar method based on lysine-sepharose affinity chromatography (Deutsch & Mertz, 1970); instead, following expression in the baculovirus system, it was purified from insect cell culture supernatants using the sequence of column chromatographic steps outlined in the Materials and methods. As seen in Figure 3, the final product was obtained at a high degree of purity; similar purity has been achieved with more than 40 mutant forms subjected to the same procedure. N-terminal sequence determination (five cycles) confirmed the expected EPLDD sequence (Sottrup-Jensen et al., 1978).

mPlg was expressed in the baculovirus system, purified, and its kinetic parameters determined; full-length *Plg* has also been expressed in this system (Whitefleet-Smith et al., 1989). The data in Table 2A,B show that, when assessed as a substrate for activation by either by *uPA* or by *mPlg-SK* complex, or by amidolysis kinetics of the *mPlm* forms, the differences between *mPlg*

[3] Although the M_r of *mPlg* is 28.4 kDa, it migrates in SDS-PAGE, in both reduced and unreduced form, at a mobility corresponding to ~37 kDa.

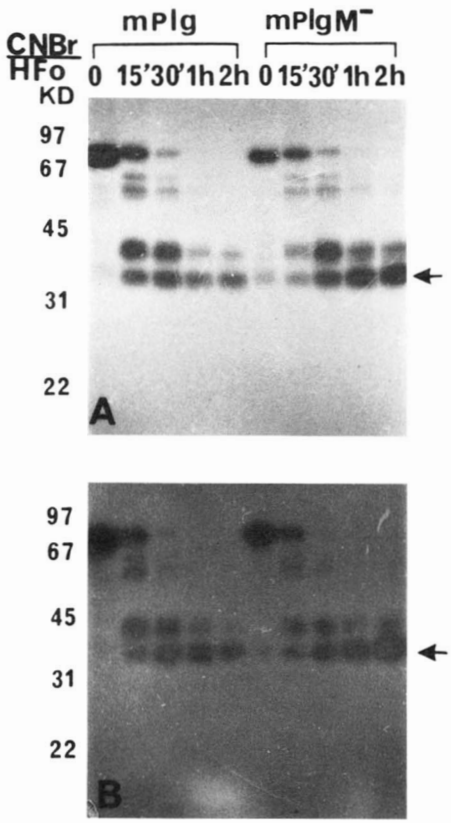

Fig. 2. Zymography of *malE-mPlg* fusion proteins. Fusion proteins were analyzed in nonreducing SDS-PAGE, after the indicated periods of incubation in CNBr/HFo, and zymography was performed according to Granelli-Piperno and Reich (1978). The indicator gel contained *uPA* (**A**) or *SK* (**B**) as activators. Arrows indicate the position of *mPlg*. Fragmentation of the fusion protein (M_r ~ 75 kDa) progressively liberates smaller sized zymographically visible bands whose activity either declines (*mPlg*, variant 1) or accumulates (*mPlgM*$^-$, variant 4) with time.

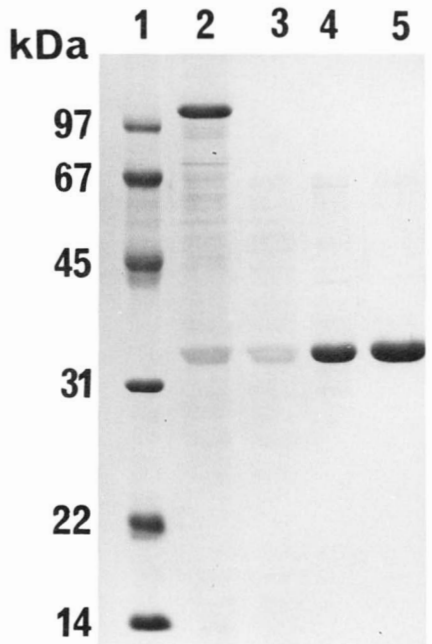

Fig. 3. Purification of *mPlg* from culture medium of High Five cells infected with recombinant baculovirus. 1, M_r markers; 2, crude culture medium; 3, flow through from DEAE-Toyopearl column; 4, eluate from heparin-Sepharose column; 5, eluate from CM-Toyopearl column. The position of the main band corresponds exactly to zymographically and immunochemically demonstrable *mPlg*. The final product has been purified 50-fold, with a yield of 70%, equal to 3–12 mg/L of original culture medium.

and *mPlgM*$^-$ were within the range of experimental variation; likewise, the differences in several *SK*-related parameters were minor (Table 2B). Thus, the consequences of M replacement appeared insignificant.

We monitored the stability of *mPlgM*$^-$ (variant 4) in CNBr/HFo to derive standardized incubation conditions applicable to site-directed proteolysis. From the esterolytic data in Figure 4 it is evident that *mPlgM*$^-$ was unaffected for the 3-h period during which the wild-type proenzyme lost 90% of its activity (the monomethionine mutants, variants 2 and 3, were inactivated at the same rate as wild-type *mPlg*); in other experiments (results not shown), essentially full activity was recovered after 5–6 h, incubation thereafter producing a slow decline (30% loss after 16 h). Taken together, the above results validated the potential of methionine shuffling to mediate site-directed proteolysis, and the procedure was extended to other constructs.

A more exacting test of the concept was provided by variant 5, where M_{29} replaced R_{29} at the activation site in the otherwise M-free protein. Confirming the observations of Davidson et al. (1990), who prepared an R → E mutant at the same position in *Plg*, this variant was no longer a substrate for *uPA*, while maintaining the capacity to form a functional activator complex with *SK* (data not shown, see Wang & Reich, 1995). Incubation in CNBr/HFo, which cleaved the mutant at the single M and produced a new N-terminal sequence identical to wild type, activated the enzyme (Fig. 5). Analysis of separate aliquots by SDS-PAGE demonstrated that the reaction mixture contained only zymogen starting material and the single expected cleavage product; no aggregates or partially degraded species were

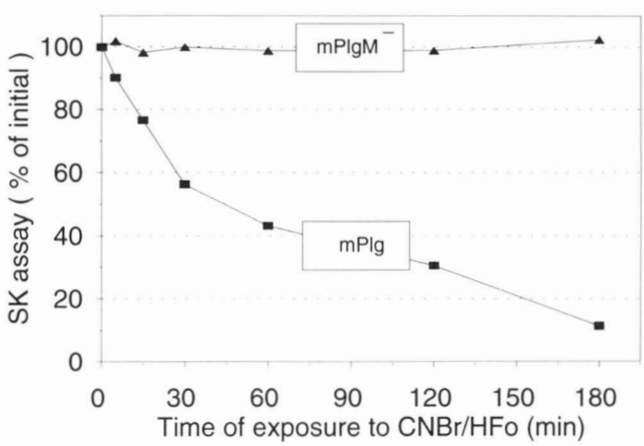

Fig. 4. *SK* assay of *mPlg* (variant 1) and *mPlgM*$^-$ (variant 4). Effect of incubation with CNBr/HFo. The M-containing protein is progressively inactivated; the M-free protein is stable.

Table 2. *Comparison of mPlg and mPlgM⁻*

	mPlg Variant 1	*mPlgM⁻* Variant 4
A. Substrate properties of *mPlg* and *mPlgM⁻*		
Activation by *uPA*		
K_m (μM)	17.1 ± 3.4	17.4 ± 2.8
k_{cat} (s^{-1})	9.5 ± 1.6	9.3 ± 1.8
k_{cat}/K_m ($\mu M^{-1}\ s^{-1}$)	0.56	0.53
Activation by *mPlg-SK* complex		
K_m (μM)	65.6 ± 9.4	61.1 ± 8.7
k_{cat} (s^{-1})	3.6 ± 0.7	2.9 ± 0.6
k_{cat}/K_m ($\mu M^{-1}\ s^{-1}$)	0.055	0.048
B. Amidolysis (S2251) by *mPlm* form		
K_m (mM)	0.336 ± 0.03	0.410 ± 0.007
k_{cat} (s^{-1})	42.7 ± 1.2	47.3 ± 2.6
k_{cat}/K_m ($mM^{-1}\ s^{-1}$)	127.1	115.4
C. Kinetic properties of *zymogen-SK* complexes		
Amidolysis (S2251) by respective *zymogen-SK* complex		
K_m (mM)	0.407 ± 0.04	0.411 ± 0.03
k_{cat} (s^{-1})	50.2 ± 2.0	44.2 ± 1.1
k_{cat}/K_m ($mM^{-1}\ s^{-1}$)	123.3	107.8
b-Plg Activation by respective *zymogen-SK* complex		
K_m (μM)	6.75 ± 1.6	6.97 ± 2.1
k_{cat} (s^{-1})	0.940 ± 0.12	0.96 ± 0.14
k_{cat}/K_m ($\mu M^{-1}\ s^{-1}$)	0.139	0.138

detected (Fig. 6). The amidolytic kinetics of this CNBr-activated mutant (with S2251 as substrate) resembled those found with *uPA* activated *mPlgM⁻* (variant 4, Table 3). Thus, plasminogen activation either by limited chemical proteolysis of variant 5, or by *uPA*-catalyzed limited proteolysis of variant 4, yielded qualitatively identical outcomes; this result further confirmed the utility of methionine shuffling as an approach to site-directed proteolysis of *mPlg*.

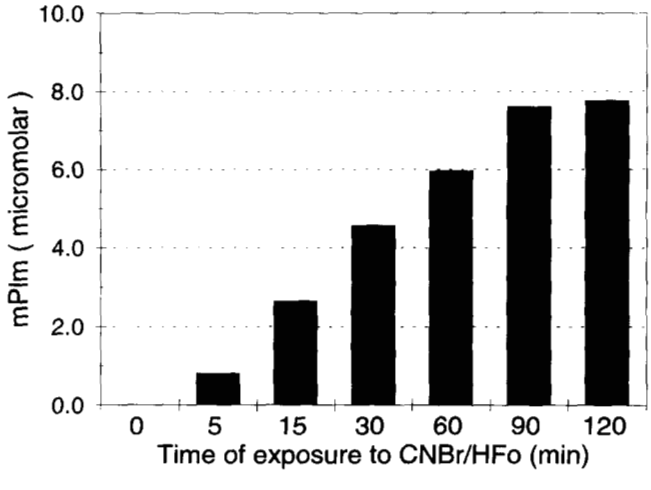

Fig. 5. Effect of CNBr/HFo on catalytic activity of variant 5 protein. Variant 5 protein, *mPlgM⁻*-M_{29}, purified as in Figure 3, was prepared and incubated in CNBr/HFo as in Figure 4. Aliquots taken at the indicated times were assayed for *mPlm* activity. *mPlm* activity appeared promptly after exposure to CNBr/HFo and increased progressively.

Proenzyme activation

The *mPlg* variants used in this study are listed in Tables 4 and 5; the positioning of mutations can be related to the protein structure by referring to Figure 1 and Table 1. Variants destined for exposure to chemical cleavage based on M shuffling were constructed in the methionineless background of variant 4 (*mPlgM⁻*); a number of these were designed to yield two different products, the results of chemical and enzymatic cleavage, respectively. All other variants, intended solely for enzymatic cleavage, were in the normal M-containing background of *mPlg* (variant 1). As shown above, these two proteins were essentially interchangeable, either as proenzymes or enzymes, with respect to substrate and catalytic activity. Mutational changes considered in this section were introduced in two regions of the protein: either within the activation loop, at or near the normal activation site (variants 5-18) (Table 4), with the aim of modifying the structure of the new N-terminal segment, or as substitutions for D_{208} (Table 5). The purified proteins were cleaved as desired to yield an *mPlm* form whose catalytic parameters

Table 3. *Comparison of variants 4 and 5*

		Variant activated by	
		4 *uPA*	5 CNBr/HFo
Amidolysis (S2251) by *mPlm* form	K_m (mM)	0.41 ± 0.07	0.46 ± 0.08
	k_{cat} (s^{-1})	47.30 ± 2.6	51.4 ± 2.9
	k_{cat}/K_m ($mM^{-1}\ s^{-1}$)	115.4	111.5

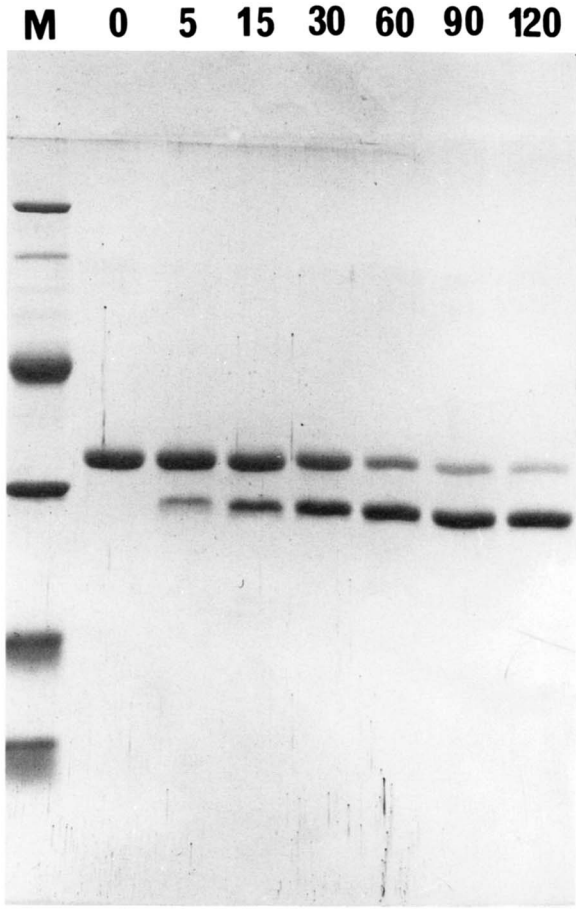

Fig. 6. Chemical proteolysis of *mPlgM*$^-$-M_{29} (variant 5). Chemical cleavage was performed as in Figure 4, and aliquots were taken at the indicated times for analysis under reducing conditions by SDS-PAGE. The single cleavage product was of the expected size; it accumulated progressively in the absence of detectable aggregates or other partial degradation products. The small *mPlm* A chain was not retained in the gel.

(K_m, k_{cat}) were assessed using a standard amidolytic and chromogenic assay procedure.

Modifications of the new N-terminal segment

The catalytic data pertaining to changes within the activation loop are tabulated in Table 4, where the variants are grouped according to the length of the new N-terminal segment located upstream of C_{34} and generated by cleavage; examples of altered amino acid composition and sequence are represented within each group.

Normal length N-termini (Table 4A). The catalytic activities of this class of *mPlm*s fall into four groups: the first consists of proteins (variants 4–6) whose new N-termini were unmodified compared to the reference structure (variant 1); the values for both K_m and k_{cat}, and, hence, the catalytic efficiencies, were very close to those for variant 1. A second group consisted of variants 7 and 8, in which a single M residue had been substituted for either V_{30} or V_{31}; here the catalytic efficiencies were lower than the reference enzyme by one to two orders of magnitude. For the third group, variants 9, 10, 13, and 14, the relative enzymatic activities were lower still, by a further one to two orders of magnitude. Finally, variant 11 was inactive when assayed as a *mPlm* alone (although activity appeared after complex formation with *SK*; see Wang & Reich, 1995).

Variants 7 and 8. With this pair of variants M has been substituted, respectively, for V_{30} and V_{31}. Compared to the normal V residue, the presence of the bulkier M side chain in either position lowered both affinity for the amidolytic substrate and k_{cat}.

Variants 9–11. Here the stepwise replacement of V_{30} by G residues has deleted one or another of the hydrophobic V side chains, or both. The two single V replacements (variants 9 and 10) were associated with substantial changes in K_m and k_{cat}, but the magnitude of the changes in catalytic constants differed significantly in the two cases. Replacement of both V by G residues (variant 11) yielded a *mPlm* that was catalytically inactive under standard assay conditions. Because both the length of the N-terminal sequence, and the position of the free NH_2 group were retained, this variant should have been capable of forming a salt-bridge with D_{208}. If that was the case, salt-bridge formation, by itself, was insufficient to accomplish proenzyme activation. Clearly, the presence of at least one V hydrophobic side chain was essential to achieve some degree of activation.

Variants 12 and 13. As might have been expected, the R_{29}–P_{30} sequence in variant 12 proved completely resistant to *uPA*-catalyzed cleavage. Variant 13 was then constructed and subjected to chemical cleavage. The resulting *mPlmP*$_{30}$ form was a surprisingly inefficient enzyme, both K_m and k_{cat} showing large differences compared to the control structure.

Variant 14. Here two bulky side chains, M_{30} and K_{31}, have been substituted for $V_{30,31}$, yielding an *mPlm* with profoundly depressed catalytic activity: approximately 600-fold lower than variant 7 (with a homologous terminal M residue) and 1.8×10^3-fold lower than variant 1.

Elongated N-termini (Table 4B). Four variants comprise this class. In the first, derived by chemical scission of variant 6, the N-terminal sequence was elongated by the addition of a single residue, R. This *mPlm* expressed no detectable amidolytic activity.

The N-termini in the remaining members of this class were elongated by one (variants 9 and 15) or two G residues (variant 11), respectively. All three expressed a similar and rather low level of activity, approximately $2–3 \times 10^3$-fold below the reference *mPlm* (variant 1), a level comparable to variant 9 (Table 2A).

Abbreviated N-termini (Table 4C). Six variants comprise this class, which includes examples of N-termini shortened by one (variants 7, 14, 16, 17) or two residues (variants 8 and 18). Whether generated by enzymatic or chemical cleavage, all of these were amidolytically inactive.

Mutations involving D_{208} (Table 5)

This remaining pair of mutant structures was designed to test whether the aspartyl residue D_{208}, and its associated salt bridge, were essential for the formation of a functional catalytic center. For one variant (variant 19), D_{208} was substituted by asparagine N_{208}. This change excluded any salt bridge, but might have allowed the formation of an H-bond with the N_{208} side-

Table 4. *Effects of changes in N-terminus on amidolytic activity of mPlm*[a]

Variant	Type of cleavage	N-terminal sequence[b]	K_m (mM)	k_{cat} (s^{-1})	k_{cat}/K_m ($mM^{-1}\ s^{-1}$)	Relative catalytic efficiency
A. Variants yielding normal-length N-termini						
1	E	V V G G	0.34 ± 0.03	42.7 ± 1.2	127.100	1.00000
4	E	V V G G	0.41 ± 0.07	47.3 ± 2.6	115.400	0.90000
5	C	V V G G	0.46 ± 0.08	51.4 ± 2.9	111.500	0.87000
6	E	V V G G	0.44 ± 0.06	49.3 ± 2.1	111.800	0.87000
7	E	M V G G	4.15 ± 0.06	16.6 ± 0.11	4.000	0.03000
8	E	V M G G	1.45 ± 0.02	1.9 ± 0.02	1.310	0.01000
9	C	V G G G	7.52 ± 1.7	0.46 ± 0.07	0.061	0.00048
10	E	G V G G	1.06 ± 0.2	0.005 ± 0.001	0.004	0.00003
11	C	G G G G	Activity undetectable[c]			
13	C	P V G G	11.3 ± 3.5	0.017 ± 0.04	0.015	0.00011
14	E	M K G G	9.63 ± 2.1	0.06 ± 0.01	0.007	0.00006
B. Variants yielding elongated N-termini						
6	C	R V V G G	Activity undetectable			
9	E	M V G G G	4.01 ± 0.4	0.16 ± 0.01	0.040	0.00031
11	E	V M G G G G	3.68 ± 0.4	0.17 ± 0.02	0.046	0.00036
15	E	V V G G G	2.12 ± 0.5	0.1 ± 0.02	0.047	0.00037
C. Variants yielding abbreviated N-termini						
7	C	V G G	Activity undetectable			
8	C	G G	Activity undetectable			
14	C	K G G	Activity undetectable			
16	E	V G G	Activity undetectable			
17	E	V V G	Activity undetectable			
18	E	V G	Activity undetectable			

[a] Variants are identified according to the numbers in Table 1. C, chemical cleavage by CNBr/73% formic acid. E, enzymatic cleavage by human urinary urokinase.
[b] The sequence upstream of C_{34} is shown for each cleavage product.
[c] But see Wang and Reich (1995).

chain carboxamide as acceptor and the N-terminal amino group as donor. The relative activity of this $mPlmN_{208}$, was reduced some 2,000-fold below *mPlm*. In the second, variant 20, D_{208} was replaced by A_{208}, a change that presumably excluded any significant side-chain interaction with the new N-terminus; the relative activity of the corresponding $mPlmA_{208}$ was very low, more than 4.1×10^4-fold lower than *mPlm* itself under the particular reaction conditions. Nonetheless, $mPlmA_{208}$ was clearly an active enzyme: the amidolysis rate enhancement was 1.7×10^4-fold that of *mPlg*, and 1.2×10^3-fold greater than the spontaneous rate of S2251 hydrolysis.[4] Though extremely feeble compared to the wild-type enzyme, both of these variant proteins expressed obvious enzymatic activity.

[4] Under standard assay conditions, the spontaneous rate of S2251 hydrolysis was 0.0995 nmol/h; the *mPlg* catalyzed rate was 0.0068 nmol/h/nmol proenzyme.

Discussion

M shuffling and chemical proteolysis

Our results show that (1) conservative replacement of all M residues can be carried out without necessarily or detectably altering the catalytic functions of *mPlg*; (2) the M-free protein can be incubated for hours without detectable loss of enzymatic activity under conditions used for M destruction and protein fragmentation, i.e., CNBr in concentrated formic acid; (3) the introduction of unique M residues provides a convenient means for reliably accomplishing site-specific, limited proteolysis to probe a number of parameters in enzyme function and protein-protein interactions.

Table 5. *Effects of substituting aspartyl$_{208}$ on amidolytic activity of mPlm*

Variant	Modification	K_m (mM)	k_{cat} (s^{-1})	k_{cat}/K_m ($mM^{-1}\ s^{-1}$)	Relative catalytic efficiency
1	Control	0.34 ± 0.03	42.7 ± 1.2	127.1000	1.00000
19	$D_{208} \rightarrow N_{208}$	3.1 ± 0.1	0.19 ± 0.03	0.0620	0.00049
20	$D_{208} \rightarrow A_{208}$	6.4 ± 0.41	0.025 ± 0.001	0.0039	0.00003

The introduction of M residues to mediate chemical cleavage at desired locations in peptide chains has been used by Wallace et al. (1991) and by Sancho and Fersht (1992).

Proenzyme activation

The cleavage products of the mutant *mPlg*s present a spectrum of enzymatic activities that is suggestive for the function of the newly formed N-terminal segment. The essential findings are:

1. From the results obtained to date, only three structural features pertaining to the new N-terminal sequence appear to be essential for proenzyme activation: a tetrapeptide sequence preceding C_{34}; at least one valine-like side chain within the terminal dipeptide; homologies within the chymotrypsinogen family suggest that a glycine residue in the fourth position is probably required, but this conclusion remains tentative, pending a definitive test. Neither the salt bridge, nor, indeed, the participating aspartic acid residue itself (D_{208}), are totally indispensable for constituting an active enzyme, though they contribute greatly to optimization of activity.

2. Judged by the catalytic activity of the respective *mPlm*s, a tetrapeptide unit preceding the disulfide bond represents both the minimal and the optimal length of the N-terminal segment. Shorter than tetrapeptide sequences (Table 4C) do not support the formation of catalytically active *mPlm*s. Some longer than tetrapeptide sequences confer activity, but at a reduced level.

3. The influence of the N-terminal segment on *mPlm* activity is a function not merely of length but also of amino acid composition: compare, e.g., the activity levels associated with the tetrapeptide sequences resulting from chemical cleavage of mutants 5, 9, 11, and 13; or the activities of the pentapeptide sequences from mutants 6 and 9, the former obtained by chemical, and the latter by enzymatic proteolysis. Bulky side chains within the terminal dipeptide or variant side chains as in mutant 13 are tolerated poorly, or not at all.

4. Structural modifications within the N-terminal segment that adversely affected amidolytic activity did so by affecting both substrate binding (K_m) and catalytic parameters (k_{cat}); these constants were influenced individually and to a variable degree by the different mutations.

These and other findings suggest a working hypothesis that is compatible with all of our observations and useful for guiding further work. The N-terminal tetrapeptide generated during *mPlg* activation is evidently essential for enzymatic activity of *mPlm* and we propose that it acts as a structural keystone in the formation of the active enzyme conformation. Once its mobility is freed from constraints by cleavage at the activation site, the tetrapeptide rotates with G_{33} (fourth from the N-terminus) acting as a swivel, enabling the terminal divaline sequence to enter a stereospecific cleft (Fig. 7). This cleft, analogous in exacting structural specificity to substrate binding sites of enzymes, is designed precisely to fit both the main-chain atoms and the divaline side chains; and the keystone function is assumed to depend principally on hydrophobic interactions involving the two valine side chains, its stability and proper positioning perhaps reinforced both by the salt bridge linking the terminal amino group to the β-carboxyl of D_{208}, and by interactions of the main chain structures. The establishment of these interactions is envisaged to impose a realignment of the surrounding structures and thereby the coordinated emergence of the two elements needed for activity—the substrate (P_1) binding site and the oxy-

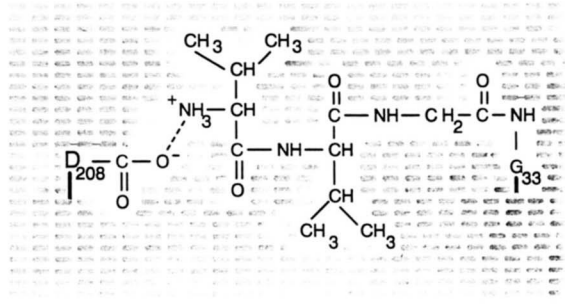

Fig. 7. Diagram illustrating the parts of the N-terminal dipeptide envisaged to interact with D_{208} and the surrounding structures after activation by chain cleavage.

anion cavity. This model of activation is consistent with the properties of variants in which: (1) valine side chains have been removed (9, 10, 11, Table 4A); (2) the N-terminal sequence has been either abbreviated (Table 4C) or extended (9, 11, 15, Table 4B); (3) bulky side chains have been placed in either of the terminal peptide positions (6, Table 4B; 7, 8, 13, 14, Table 4A). The activity profile of our mutants implies that the restructuring needed for enzyme activation is likely to be a subtle process.

Finally, we note that, compared to the reference enzymes, every modification in new N-terminal structure impaired both K_m and k_{cat} (Table 4). This would be expected if, as we postulate, the substrate binding site and the catalytic assembly appear coordinately following a realignment provoked by the insertion of the N-terminus; any deviation from the reference structure would influence both functions. It is likely that the overall catalytic sequence (reflected in k_{cat}) would be more exacting in its structural requirements and hence more sensitive to minor perturbations of the enzyme's functional group architecture, than the formation of the enzyme–substrate complex. More detailed enzymological studies combined with crystallographic analysis of our mutant structures might be revealing both of catalytic mechanism and proenzyme activation.

The N-terminal sequences of all other known members of the chymotrypsin(ogen) family resemble *Plg* in having a G at the fourth position downstream of the N-terminus, as well as two alkyl side chains of moderate size in the terminal dipeptide; and several proenzymes, like *Plg*, have a second G at the third position; hence their termini are likely to function in a manner similar to that of *mPlg*.

Our hypothesis is in accord with previous studies of related serine proteases: it provides a functional explanation for the crystallographically observed differences between chymotrypsin and trypsin and their respective zymogens (Freer et al., 1970; Birktoft & Blow, 1972; Fehlhammer et al., 1977; Kossiakoff et al., 1977; Huber & Bode, 1978); and it dovetails with the reports by Bode (1979) and others (Bode et al., 1978) showing that a combination of very tightly binding inhibitors and high concentrations of N-terminal dipeptide could force trypsinogen into a trypsin-like, though catalytically inactive, conformation.

Materials and methods

All reagents were obtained from regular commercial sources and were of the best analytical or molecular biology grade available.

Streptokinase was generously provided by Hoechst-Roussel Pharmaceuticals Inc., Somerville, New Jersey, and by Lederle Laboratories, Pearl River, New York.

Human urinary urokinase was obtained from Laboratoires Serono, Aubonne, Switzerland.

Construction and cloning of mPlg

All procedures related to recombinant material were performed using standard methods (Sambrook et al., 1989). All DNA fragments were produced using PCR and oligonucleotide primers of appropriate sequence centered on unique restriction sites. Human full-length plasminogen cDNA, cloned in pBS (Stratagene), was obtained in plasmid form from Dr. Sandra Degen (Children's Hospital Research Foundation, Cincinnati, Ohio) grown in *E. coli*, the plasmid isolated and used to generate two fragments by PCR. The first, shorter fragment, contained flanking nonspecific hexanucleotide sequences at both ends enclosing unique flanking restriction sites (*Xba* I, *Nhe* I, *Xho* I at the 5′ end, and *Bsu* 36I at the 3′ end) and nucleotide sequence coding for the signal sequence for secretion and the first 11 amino acids of mature glu-plasminogen (to G_{11}) and a further 8 residues, beginning at P_{544} of *Plg* and terminating at P_{19} of *mPlg* (P_{551} of *Plg*) corresponding to the *Bsu* 36I site. The second, large fragment contained the nucleotide sequence coding for amino acids P_{551}–N_{791} of mature plasminogen (P_{19}–N_{259} of *mPlg*, i.e., the proenzyme domain), termination codon, again with flanking hexanucleotides, and reciprocal unique restriction sites (*Bsu* 36I at 5′, and *Xba* I, *Nhe* I, and *Xho* I at 3′ end). Concurrently, a unique *Xma* I site was introduced (by PCR) without change in amino acid sequence at a position corresponding to the P_{27}–G_{28} sequence immediately preceding the R_{29} residue at the activation site of *mPlg*. The two fragments were ligated at the *Bsu* 36I site, the resulting *mPlg*-cDNA cloned into the *Xba* I site of pUC 19, and the nucleotide sequence determined using the dideoxy method (Sambrook et al., 1989). The insert was then transferred into pJVP10Z using the *Nhe* I sites. For cloning into *pMal-p* the *mPlg* sequence was again amplified in a separate PCR run using a primer that inserted a *Bam*H I site at the 5′ end and a methionine residue at the *malE–mPlg* junction; this product was then cloned into *pMal-p* using the *Bam*H I and *Xba* I sites. Two unique restriction sites – *Xma* I and *Rsr* II – provided a convenient cassette for inserting analogous, mutant fragments in proper orientation into *pMal-p* and pJVP10Z. Subsequently, additional unique sites were introduced (*Bam*H I, *Hga* I, *Ppu*M I) without modifying protein sequence. An abbreviated map indicating unique restriction sites is shown in Figure 8. (Note: *Bam*H I, *Hga* I, and *Ppu*M I were not present in all constructs; there are two *Ban* II sites.)

The sequence of all mutant constructs was verified by sequencing the recombinant *pMal-p*, pJVP10Z, and baculovirus DNAs.

Production of variant genomes

All variant sequences were produced in appropriately primed PCR reactions, with each primer designed to be compatible with one of the unique restriction sites in *mPlg*, and a suitable *mPlg* fragment as template. The primer sequences (shown 5′ → 3′, left to right) were as follows:

1. att aat tct aga gct agc ctc gag tcc caa aat gga aca taa gga agt
2. att aat cct gag gct tcc cac aat caa atg agg gcc cct ggg tat tca cat agt ca
3. att aat cct cag gtt gaa cct aag aaa tgt ccc ggg agg gt
4. att aat tct aga gct agc ctc gag tta att att tct cat cac tcc ct
5. att aat gga tcc atc gag ggt agg cct atg gac gac tat
6. att aat ggt gcc tcc aca gaa gtg ctg tcc aaa
7. att aat tct aga gct agc ctc gag tta att att tct caa cac tcc ctc
8. att aat ccc ggg atg gtt gtt gga gga tgt gtg g
14. att aat tgt ccc atg cgc gtc gtt gga g
15. att aat gac gcg cat ggg aca ttt ctt agg
20. att aat ccc ggg aga gtt gga ggt tgt gtg gcc cac
21. att aat ccc ggg aga gtt gtg gga tgt gtg gcc cac
22. att aat ccc ggg aga gtt gga tgt gtg gcc cac
23. att aat gac gcg ttg ttg gag gat gtg tgg ccc acc cac
24. att aat cct cca aca acg cgt ccg gga cat ttc tta gg
25. att aat gac gcg ttg ttg gag gag gat gtg tgg
26. att aat ccc ggg cgc atg gtt ggt gga gga tgt
27. att aat ccc ggg cgc gtt atg ggt ggt gga gga tgt
28. att aat ccc ggg agg ggt gtt gga gga tgt gt
29. att aat ccc ggg agg cct gtt gga gga tgt gtg g
30. att aat ccc ggg agg atg aaa gga ggt tgt gtg gcc ga
31. att aat ccc ggg cgc atg gtt gga gga tgt gt
32. att aat ccc ggg cgc gtc atg gga gga tgt gt
33. att aat ccc ggg atg cct gtt gga gga tgt gtg g
34. att aat gag gtc ctc tgg ttt gct tcg aga ag
35. att aat agg acc tcc act att acc ctg gca act g
36. att aat agg acc tcc act agc acc ctg gca act g

Primers 1 and 2 were used for the shorter PCR fragment of *mPlg*; 3 and 4 for the larger *mPlg* fragment; 5 was for cloning of *mPlg* into pMal-p at *Bam*H I site(5′) in combination with 4 (3′, *Xba* I site); 6 was for $M_{56} \rightarrow Q_{53}$ mutation; 7 for $M_{256} \rightarrow L_{256}$; 8 was used for $R_{29} \rightarrow M_{29}$ change.

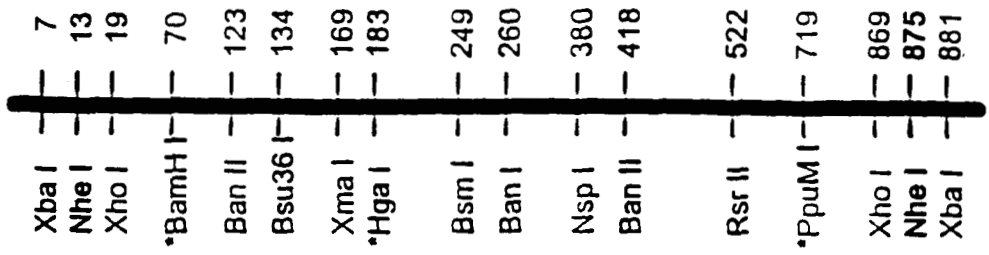

Fig. 8. Unique restriction sites used in construction and cloning of *mPlg*. See Materials and methods for details.

Primers 14 and 15 were for variant 6; primer 31 for variant 7; 32 for variant 8; 26 for variant 9; 28 for variant 10; 27 for variant 11; 29 for variant 12; 33 for variant 13; 30 for variant 14; 25 for variant 15; 19, 20, and 21 for variants 16, 17, and 18; 35 and 36, together with oligo 34, for variants 19 and 20. Primers 23 and 24 were used to create a *Hga* I site. All variant sequences were verified by DNA sequencing of recombinant *pMal-p*, pJVP10Z, and baculoviral DNAs.

Eukaryote expression, mediated by recombinant baculoviruses, in insect cells

Here we have used a transfer plasmid (pJVP10Z) developed by Richardson (Vialard et al., 1990) and generously provided by him. It contains a β-galactosidase insert that identifies recombinant plaques by a deep blue color when the chromogenic substrate X-gal is present in the agar overlay. Conditions for growth and transfection of Sf9 cells, preparation of virus, and viral DNA were as described by Miller et al. (1986), whereas those for the chromogenic plaque assay were according to Summers and Smith (1987). Where feasible, concurrent expression of functional *mPlg* was monitored in the absence of X-gal, using the same principle as in zymography, by incorporating *SK* (500 μ/mL), casein (10 mg/mL medium) to opacify the agar overlay, replacing the serum by acidified serum, and adding a supplement of bovine *Plg* (10 μg/mL). The serum component in the plaque assay being of fetal bovine origin, its plasminogen is not activated by "human" *SK*, and the overlay remains opaque in the absence of human *mPlg* whose expression within a recombinant plaque is visible as a concentric lytic zone. Plaques were picked and replated until a pure recombinant baculovirus clone was obtained. The lytic plaque technique could not be used for mutant proteins having low catalytic activity.

For preparative scale isolation of *mPlg*, nearly confluent monolayer cultures of High Five cells, grown in Ex401 medium (JRH Biosciences) under serum-free conditions in T175 flasks, were infected at a multiplicity of >5 pfu/cell; monolayers were maintained for 3–4 days in the absence of serum, *mPlg* concentration in the medium being monitored at intervals. When a plateau concentration was reached (usually ~15 μg/mL), the culture medium was collected (100–500 mL), cleared of cellular debris by centrifugation (4,000 × *g*, 10 min) in the cold, dialyzed against 10 mM Na cacodylate buffer, pH 7.0, and applied to a DEAE-Toyopearl column (2.5 × 18 cm) connected in tandem to a column (2.5 × 10 cm) of heparin-agarose equilibrated with the same buffer; most of the proteins adsorbed to the DEAE column; *mPlg* passed through and adsorbed to the heparin-agarose. The latter was washed and *mPlg* eluted with cacodylate (10 mM, pH 7.0, 120 mM NaCl). The *mPlg* fraction was then dialyzed to cacodylate (10 mM, pH 7.0) and loaded onto a column of CM-Toyopearl (2.5 × 6 cm) equilibrated with the same buffer; *mPlg* was eluted with a salt gradient (0–0.3 M NaCl, in cacodylate pH 7.0, 10 mM, 160 mL total) in highly purified form. The overall recovery was ~70–80% with a yield of about 3–12 mg/L of original culture medium. The purified protein was dialyzed against sodium acetate (0.5 mM, pH 7.0) and lyophilized.

Enzyme assay

Except where indicated to the contrary, all enzyme assays were performed using the esterolytic system described by Green and Shaw (1979), with the substrate, *Z*-lys-thiobenzyl ester and the chromogen 5-5′-dithiobis-(2-nitrobenzoic acid) at 0.11 mM and 0.32 mM final concentrations, respectively. All assays were standardized to ensure linearity with enzyme concentration and time of incubation. All proteins were dissolved and diluted in PBS containing acid-treated BSA (1 mg/mL).

SK assay

This assay was used for all routine testing and monitoring and was conducted at a single final concentration of SK (3,000 μ/mL) that was saturating for *mPlm*s but not for *mPlg*s. All *mPlg*s were dissolved in PBS-BSA on ice, at concentrations of 0–15 nM; the *SK* was dissolved in PBS at 4,000 μ/mL. To 100 μL of *mPlg* was added 300 μL of *SK* and the mixture incubated at 37 °C for 10 min; 10 μL of a solution containing the substrate and chromogen were then added, the reaction allowed to proceed for 5 min at 37 °C (up to 30 min for low activity variants) and terminated by the addition of a large excess of basic pancreatic trypsin inhibitor (Trasylol, aprotinin); the optical density at 412 nm was recorded.

mPlm activity assay

The Green and Shaw esterolytic assay (Green & Shaw, 1979) was used to determine *uPA* activation kinetics by measuring the *mPlm* produced from each of the mutant *mPlg*s, except for certain variants, whose low *mPlm* activity did not permit *uPA* parameters to be defined. The *mPlm*s were in PBS-BSA as for the *SK* assay, at final concentrations of 0–5 nM. To 400 μL of *mPlm* solution was added 10 μL containing the substrate-chromogen mixture, and the reaction was incubated at 37 °C for 5 min. The assay was adapted to accommodate the catalytic levels of the less active variants either by increasing the enzyme concentration, prolonging the incubation period, or both. These were as follows: for variant 7, 1 nM enzyme protein, 5–30 min incubation; for variant 8, 2 nM, 5–30 min; for variant 9, 70 nM, 10–60 min; for variants 10, 13, 14, 15, 19, 20, 150 nM, 20–120 min.

Preparation of mPlm for assay

The various *mPlg*s were dissolved at a concentration of 20 μM in PBS containing 25% glycerol; *uPA*, dissolved in the same solvent was added to a final concentration of 200 nM, the mixture incubated for 12 min at 37 °C, and the reaction terminated by rapid cooling. Aliquots were withdrawn for active site titration according the Chase and Shaw (1970), for amidolysis assay, and for *mPlm* activity assay.

Amidolysis assay

This assay (Friberger et al., 1978), with Kabi compound S2251 (0.1–5 mM) as substrate, was used to determine the amidolytic kinetics of *mPlm*s and *mPlg-SK* complexes. The values of K_m and k_{cat} were determined by the Lineweaver–Burk method, in PBS at 37 °C.

The enzyme concentrations used were: for *mPlm*s, 0.2 nM; for *mPlg-SK* complexes, 0.2 nM for variants 1 and 4, and 2.0 nM for variant 5. Incubation was at 37 °C for 5–30 min; the reaction was terminated by addition of acetic acid and the optical density recorded at 405 nm. To prepare the *mPlg-SK* complexes, 50 μL of a solution of each mutant *mPlg* (20–40 μM in PBS) were mixed with 100 μL of a solution of SK (20 μM in the same buffer), incubated at 37 °C for 10 min, rapidly cooled, and maintained on ice. The complexes were then assayed for active site concentration and

amidolytic activity (S2251 substrate) under exactly the same conditions as the *mPlms*. The complexes were also assayed in a plasminogen activation reaction with *b-Plg* as substrate (see below).

To determine the spontaneous as well as the *mPlg*-catalyzed rate of amidolysis, S2251 (5 mM in PBS), in the presence and absence of *mPlg* (10 μM), was incubated under sterile conditions in tightly capped reaction tubes at 37 °C. Aliquots were taken at 40-h intervals and the optical density at 405 nm was measured in the usual way.

Kinetics of mPlg activation by uPA and by mPlg-SK complex

The assays were performed in PBS, at 37 °C for 0–20 min, and the results were calculated by the Lineweaver–Burk method. The *mPlg* substrate concentration range was 2.0–50 μM for *uPA*, and 2.0–20 μM for *mPlg-SK* complex. The final concentration of *uPA* was 0.1 nM; the final concentration of *mPlg-SK* complex was 0.5 nM. The *mPlm* products were assayed in the *mPlm* activity assay as described above.

Activation of b-Plg by mPlg-SK complexes

The kinetics of *b-Plg* activation by *mPlg-SK* complexes were determined in PBS, at 37 °C, with *b-Plg* in the concentration range 1.67–13 μM; incubation times were 0–20 min. The *variant 4-SK* and *variant 1-SK* complexes were used at 0.5 nM, and *construct 5-SK* at 10.0 nM final concentration, respectively. The resulting *b-Plm* was diluted in PBS-BSA and assayed in the standard *mPlm* assay. *b-Plg* was isolated from calf serum using the procedure of Deutsch and Mertz (1970).

Chemical cleavage of M-containing proteins

The proteins (approximately 100 μg), purified as described and lyophilized, were redissolved in 50 μL of 73.5% formic acid containing 5 mg/mL tryptophan; to 45 μL of this solution was added 5 μL of a solution of CNBr (400 mg/mL in formic acid–tryptophan) and the mixture incubated at 23 °C for the desired periods. The reaction (usually 5-μL aliquots) was terminated by the addition of DL-methioninamide (10 mg/mL final concentration), the mixture evaporated to dryness in a stream of nitrogen, the residue dissolved in 90 μL of PBS, and activity measured in the indicated assay.

Acknowledgments

We thank Andrea Fernandes for technical assistance, W. Mangel and J. Manning for helpful suggestions, F.M. Huennekens for comments on the manuscript, and Ciba-Geigy, A.G., Basle, Switzerland for financial support. This work was supported in part by National Institutes of Health grant 5 RO1 HL50320-01.

References

Birktoft JJ, Blow W. 1972. Structure of crystalline chymotrypsin. V. The atomic structure of tosyl-chymotrypsin at 2 Å resolution. *J Mol Biol 68*(2):187–240.

Bode W. 1979. The transition of bovine trypsinogen to a trypsin-like state upon strong ligand binding II. The binding of the pancreatic trypsin inhibitor and of isoleucine-valine and of sequentially related peptides to trypsinogen and to *p*-guanidinobenzoate-trypsinogen. *J Mol Biol 127*(4): 357–374.

Bode W, Schwager P, Huber R. 1978. The transition of bovine trypsinogen to trypsin-like state upon strong ligand binding. The refined crystal structures of the bovine trypsinogen-pancreatic trypsin inhibitor complex and of its ternary complex with Ile-Val at 1.9 Å resolution. *J Mol Biol 118*(1): 99–112.

Chase TJ, Shaw E. 1970. Titration of trypsin, plasmin, and thrombin with *p*-nitrophenyl *p'*-guanidinobenzoate HCl. *Methods Enzymol 9*:20–27.

Davidson DJ, Higgins DL, Castellino FJ. 1990. Plasminogen activator activities of equimolar complexes of streptokinase with variant recombinant plasminogens. *Biochemistry 29*(14):3585–3590.

Deutsch DG, Mertz ET. 1970. Plasminogen: Purification from human plasma by affinity chromatography. *Science 170*(962):1095–1096.

Fehlhammer H, Bode W, Huber RJ. 1977. Crystal structure of bovine trypsinogen at 1.8 Å resolution. II. Crystallographic refinement, refined crystal structure and comparison with bovine trypsin. *J Mol Biol 111*(4): 415–438.

Freer ST, Kraut J, Robertus JD, Wright HT, Xuong NH. 1970. Chymotrypsinogen: 2.5-angstrom crystal structure, comparison with alpha-chymotrypsin, and implications for zymogen activation. *Biochemistry 9*(9): 1997–2009.

Friberger P, Knös M, Gustavsson S, Aurell L, Claeson G. 1978. Methods for determination of plasmin, antiplasmin and plasminogen by means of substrate S-2251. *Haemostasis 7*:138–145.

Granelli-Piperno A, Reich E. 1978. A study of proteases and protease-inhibitor complexes in biological fluid. *J Exp Med 148*(1):223–234.

Green GDJ, Shaw E. 1979. Thiobenzyl benzyloxycarbonyl-lysinate, substrate for a sensitive colorimetric assay for trypsin-Like enzymes. *Anal Biochem 93*:223–226.

Gross E, Witkop B. 1961. Selective cleavage of the methionyl peptide bonds in ribonuclease with cyanogen bromide. *J Am Chem Soc 83*:1510–1511.

Huber R, Bode W. 1978. Structural basis of the activation and action of trypsin. *Acc Chem Res 11*:114–122.

Kossiakoff AA, Chambers JL, Kay LM, Stroud RM. 1977. Structure of bovine trypsinogen at 1.9 Å resolution. *Biochemistry 16*(4):654–664.

Miller DW, Safer P, Miller L. 1986. An insect baculovirus host-vector system for high level expression of foreign genes. In: Setlow JK, Hollaender A, eds. *Genetic engineering, principle and methods, vol 8*. New York: Plenum Press. pp 277–298.

Riggs PD. 1990. Expression and purification of maltose-binding protein fusions. In: Ausubel FM et al., eds. *Current protocols in molecular biology*. New York: Greene Publishing Associates/Wiley Interscience.

Sambrook J, Fritsch EE, Maniatis T. 1989. *Molecular cloning: A laboratory manual*. Cold Spring Harbor Laboratory, New York: Cold Spring Harbor Laboratory Press.

Sancho J, Fersht AR. 1992. Dissection of an enzyme by protein engineering the N and C-terminal fragments of barnase form a native-like complex with restored enzymic activity. *J Mol Biol 224*:741–747.

Shi GY, Wu HL. 1988. Isolation and characterization of microplasminogen. A low molecular weight form of plasminogen. *J Biol Chem 263*(32): 17071–17075.

Sottrup-Jensen L, Claeys H, Zajdel M, Petersen TE, Magnusson S. 1978. The primary structure of human plasminogen: Isolation of two lysine binding fragments and one miniplasminogen (MW, 38,000) by elastase-catalyzed-specific limited proteolysis. In: Davidson JF, Rowan RM, Samama MM, Desnoyers PC, eds. *Progress in chemical fibrinolysis and thrombolysis, vol 3*. New York: Raven Press. pp 191–209.

Summers M, Smith GE. 1987. *A manual of methods for baculovirus vectors and insect cell culture procedures*. Texas Agricultural Experiment Station.

Vialard J, Lalumiere M, Vernet T, Briedeis D, Al-khatib G, Henning D, Levin D, Richardson C. 1990. Synthesis of membrane fusion and hemagglutinin proteins of measles virus, using a novel baculovirus vector containing the beta-galactosidase gene. *J Virol 64*(1):37–50.

Wallace CJA, Guillemette JG, Hibiya Y, Smith M. 1991. Enhancing protein engineering capabilities by combining mutagenesis and semisynthesis. *J Biol Chem 266*(32):21355–21357.

Wang J, Reich E. 1995. Structure and function of microplasminogen: II. Determinants of activation by urokinase and by the bacterial activator streptokinase. *Protein Sci 4*:1768–1779.

Whitefleet-Smith J, Rosen E, McLinden J, Ploplis VA, Fraser MJ, Tomlinson JE, McLean JW, Castellino FJ. 1989. Expression of human plasminogen cDNA in a baculovirus vector-infected insect cell system. *Arch Biochem Biophys 271*(2):390–399.